

# Improved Protocol for Single Nucleus RNA-sequencing of Frozen Human Bladder Tumor Biopsies

Sofie S. Schmøkel<sup>1,2</sup>, Iver Nordentoft<sup>2</sup>, Sia V. Lindskrog<sup>1,2</sup>, Philippe Lamy<sup>2</sup>, Michael Knudsen<sup>2</sup>, Jørgen Bjerggaard Jensen<sup>1,3</sup>, Lars Dyrskjøt<sup>1,2,4</sup>

<sup>1</sup>Department of Clinical Medicine, Aarhus University, Aarhus, Denmark.

<sup>2</sup>Department of Molecular Medicine, Aarhus University Hospital, Aarhus, Denmark.

<sup>3</sup>Department of Urology, Aarhus University Hospital, Aarhus, Denmark.

<sup>4</sup> Lead contact. Correspondence: [lars@clin.au.dk](mailto:lars@clin.au.dk) (LD)

## Abstract

This paper provides a laboratory workflow for single nucleus RNA-sequencing (snRNA-seq) including a protocol for gentle nuclei isolation from fresh frozen tumor biopsies, making it possible to analyze biobanked material. To develop this protocol, we used non-frozen and frozen human bladder tumors and cell lines. We tested different lysis buffers (IgePal and Nuclei EZ) and incubation times in combination with different approaches for tissue and cell dissection; sectioning, semi-automated dissociation, manual dissociation with pestles, and semi-automated dissociation combined with manual dissociation with pestles. Our results showed a combination of IgePal lysis buffer, tissue dissection by sectioning and short incubation time was the best conditions for gentle nuclei isolation applicable for snRNA-seq, and we found limited confounding transcriptomic changes based on the isolation procedure. This protocol makes it possible to analyze biobanked material from patients with well described clinical and histopathological information and known clinical outcomes with snRNA-seq.

Keywords: nuclei isolation, single nucleus RNA-sequencing, single nuclei RNA-sequencing, single cell RNA-sequencing, single cell analysis, drop-seq, dronc-seq, 10x chromium, bladder cancer

## Introduction

The field of single cell genomics has developed rapidly during the last years and allows investigation of tissue at single cell resolution. Single cell RNA-sequencing (scRNA-seq) has been used to identify novel cell types and cell states<sup>1,2</sup>. Furthermore, the method has also been used to reveal the composition of the tumor ecosystem in e.g. metastatic melanoma, and to detect rare cell subpopulations and unravel intra-tumor heterogeneity<sup>2-6</sup>. However,

frequently applied protocols for scRNA-seq require single cell suspensions from fresh tissue isolated directly from surgery, which is often a confined resource and limits the use of clinically well-defined specimens. In addition, duration of surgery is often unknown and maintenance of tissue integrity following tissue resection is not prioritized and further challenges scRNA-seq with a laboratory protocol requiring a minimum of eight hours laboratory work<sup>7,8</sup>. Furthermore, clinical information, treatment response and outcome of the patients are unknown at the time of tissue procurement, and hence expensive and often unnecessary analyses of tumors, not relevant for the study in question, are carried out. In contrast, single nucleus RNA-sequencing (snRNA-seq) makes it possible to investigate fresh, fixed, or frozen tissue using e.g. the DroNc-seq method, a massively parallel snRNA-seq droplet-based technology, developed by Habib et al.<sup>7</sup>.

snRNA-seq facilitates hypothesis-generating studies and analysis of histologically well-characterized tumor biopsies from patients with long-term clinical follow up. From a practical point of view, the snRNA-seq method benefits from short processing time compared to scRNA-seq methods and experiments can be carried out when needed. There is a risk of bias when isolating whole tumor cells due to differences in the composition of tumor specimens and the robustness of the cell membrane of tumor cells. This bias is diminished by nuclei isolation because the nuclear membrane is more robust<sup>9</sup>. In addition, it is possible to isolate single nuclei from tissues, where single cell isolation may be difficult<sup>10</sup>. However, we have not found previously published protocols for nuclei isolation<sup>11,12</sup> applicable for both healthy and cancerous bladder tissue, nor adequately gentle for isolation of nuclei at a healthy state to maintain integrity of the RNA.

Here, we describe the full workflow, from frozen tumor biopsies to snRNA-seq data. The workflow includes a protocol for gentle unbiased nuclei isolation from fresh frozen human bladder tumor biopsies followed by DroNc-seq analysis and optimized library preparation for next generation sequencing. The protocol is robust and highly reproducible across various tumor stages and tumor morphology structures.

## Materials and methods

### Patient samples and processing

Bladder tumor samples were obtained from patients diagnosed with non-muscle invasive bladder cancer or muscle invasive bladder cancer. All patients had provided written informed consent to participate in future research projects before inclusion. The study was approved by The National Committee on Health Research Ethics (#1706291 & #1708266). Tumor samples were obtained from transurethral resection of the bladder or radical cystectomy.

Seven biopsies were processed fresh directly from surgery, 57 samples were embedded in O.C.T., frozen in liquid nitrogen and subsequently stored at -80 °C, and 19 samples were dry frozen in liquid nitrogen without O.C.T. and stored at -80 °C. The tumors represented various tumor stages (31 Ta; 27 T1; 25 T2-4) and tumor grades (26 low grade; 54 high grade; 3 unknown grade).

### **Cell culture**

Human bladder cancer cell line T24 was obtained from American Type Culture Collection (ATCC-LGC standards, Borås, Sweden) and re-authenticated via STR analysis using the Cell-ID-system (G9500, Promega, Nacka, Sweden). Murine embryonic fibroblast cell line, NIH 3T3, were provided by C. Holmberg, University of Copenhagen, Denmark. Both cell lines were cultivated in Dulbecco's Modified Eagle Medium (DMEM) (Lonza, cat #BE13-604F) supplemented with 10% Fetal Bovine Serum (FBS) (Gibco, cat #10270-106) and 1% penicillin/streptomycin (Gibco, cat #15140-122) and cultured at 37 °C, 5% CO<sub>2</sub> and 90% humidity to a confluence of 70-90%.

### *Preparation of Cell Lines for Nuclei Isolation for Nuclei Concentration Analysis and DroNc-seq Experiments*

T24 cells and NIH 3T3 cells cultured in separate flasks were washed with 1x PBS (Life Technology, cat #BE17-512F), and treated with 0,05% Trypsin-EDTA (1X) (Gibco, cat #25300-062) for 3-5 min. Trypsin was neutralized with 3 mL of growth medium, and the suspensions were spun down at 500× g for 5 min. at 4 °C. Supernatant was removed, the pellets were washed with 3 mL PBS, and spun down again at 500× g for 5 min. at 4 °C. Following, the supernatant was removed.

### **Nuclei isolation**

Below, two protocols for nuclei isolation are described. The first protocol describes isolation of nuclei from cell lines for nuclei concentration analysis. This protocol was too harsh for tumor tissue, so a second protocol for nuclei isolation was developed. The second protocol describes isolation of nuclei from T24 human bladder cancer cell line and human muscle invasive and non-muscle invasive bladder tumors prior to DroNc-seq. This latter protocol is more gentle.

#### *Nuclei isolation for nuclei concentration analysis*

The T24 and NIH 3T3 cell pellets were dissolved in 4 mL ice-cold Nuclei EZ lysis buffer (Sigma Aldrich, cat #NUC-101) and incubated on ice for 5 min. The suspension was centrifuged at 500× g for 5 min. at 4 °C, the supernatant was removed and the pellet

resuspended in 4 mL Nuclei Suspension Buffer 1 (NSB1; 1x PBS, 0.01% BSA (New England Biolabs, cat #B9000S) and 0.5 U per  $\mu$ L RNase inhibitor (Nordic Biolabs, cat #30281-1)). The suspension was centrifuged at 500 $\times$  g for 5 min. at 4 °C, and the supernatant was discarded. The nuclei were resuspended in 2 mL NSB1, and filtered through a 20  $\mu$ M cell strainer (pluriSelect, cat #43-10020-40). 10  $\mu$ L of each nuclei suspension was stained with 10  $\mu$ L Trypan Blue Solution 0.4% (Roche, cat #5650640001), loaded on a Bürker-Türk counting chamber, and evaluated under a microscope to ensure properly isolated, good-looking single nuclei. For the nuclei concentration analysis using DroNc-seq, the nuclei suspensions were diluted in NSB1 to concentrations of 450,000 nuclei per mL, and 500,000 nuclei per mL, and the two cell specimens were mixed 1:1 before they were loaded to the DroNc-seq system.

#### *Nuclei isolation for DroNc-seq and 10x Chromium*

Nuclei from a T24 cell line and human bladder tumor biopsies for DroNc-seq experiments were isolated with IgePal lysis buffer (50 mM Tris-HCl pH 8.5 (Sigma Aldrich, cat #T3253-100G), 150 mM NaCl (EMD Millipore, cat #106406), and 1% IGEPAL® CA-630 (Sigma Aldrich, cat #I8896)). Tumor biopsies were sectioned into 50  $\mu$ M sections on a cryostat. The remaining protocol is identical for T24 cell line and bladder tumor biopsies used for nuclei isolation for DroNc-seq and 10x Chromium. A pellet of T24 cells or sections of tissue were placed in a tube with 5 mL ice cold IgePal lysis buffer and incubated for 3-5 min. The suspension was filtered through a 70  $\mu$ M cell strainer (Corning, cat #431751) followed by a 50  $\mu$ M cell strainer (CellTrics, cat #04-004-2327). Nuclei were collected by centrifugation at 500 $\times$  g for 5 min. at 4 °C. The nuclei were washed in 4 mL Nuclei Suspension Buffer 2 (NSB2; 1x PBS, 0.05% BSA, 0.5 U per  $\mu$ L RNase inhibitor and 1 mM DL-Dithiothreitol solution (Sigma Aldrich, cat #43816)), filtered through a 40  $\mu$ M cell strainer (Flowmi, cat #15342931) and collected at 500 $\times$  g for 5 min. at 4 °C. The supernatant was removed and the isolated nuclei was resuspended in an appropriate amount of NSB2. 10  $\mu$ L of the nuclei suspension was stained with 10  $\mu$ L DAPI (Invitrogen, cat #D21490), loaded on a Bürker-Türk counting chamber, and evaluated under a fluorescence microscope to ensure properly isolated, good-looking singletions. The nuclei were counted and diluted in NSB2 to a final concentration of 453,000 nuclei per mL for DroNc-seq experiments and 1,000 nuclei per  $\mu$ L for 10x Chromium experiments.

For optimization and comparable experiments of protocols for nuclei isolation, nuclei were also isolated using Nuclei EZ lysis buffer combined with tissue dissectioning by mechanical dissociation with dounce homogenizers (Sigma Aldrich, cat #D8938), semi-automated dissociation with gentleMACS Octo Dissociator with Heaters (Miltenyi Biotec, cat

#130-096-427), and a combination of mechanical and semi-automated tissue dissectioning (supplementary table 1, supplementary figure 1).

This protocol utilizing IgePal lysis buffer for nuclei isolation was the most gentle and efficient protocol regarding highest number of nuclei isolated in relation to minimal use of tissue, reduced processing time, minimized RNA degradation, and visibly good-looking nuclei isolated.

### **Bulk mRNA analysis**

T24 cells, tissue sections from a human bladder tumor biopsy, and nuclei, from same batch of both, isolated as described above, were lysed and total RNA purified using RNeasy Mini Kit (Qiagen, cat #74106). mRNA was isolated from 500 ng total RNA using KAPA mRNA Capture Kit (KAPA Biosystems, cat #KK8441), and next generation sequencing libraries were constructed using KAPA mRNA HyperPrep Kit (KAPA Biosystems, cat #KK8544).

Bulk RNA libraries were sequenced on the Illumina NovaSeq 6000 platform using cycle parameters Read 1: 150 bases, Index read 1: 8 bases, Index read 2: 8 bases and Read 2: 150 bases. Salmon<sup>19</sup> was used to quantify the expression of transcripts using annotation from the Gencode release 33 on genome assembly GRCh38. Transcript-level estimates were imported and summarized at gene-level using the R package tximport v1.20.0 and counts were normalized using the R package edgeR v3.34.1.

### **Microfluidic system for DroNc-seq and Drop-seq**

To encapsulate nuclei with barcoded beads for DroNc-seq analysis, the Dolomite Bio scRNA-seq system (Dolomite Bio, cat #3200538) with high-speed digital microscope and camera (Dolomite Bio, cat #3200531), and sNuc-seq Chip (85 $\mu$ m Etch Depth, Dolomite Bio, cat #3200607) was used. A loading concentration of 450,000 nuclei per mL and 500,000 nuclei per mL was used for the nuclei concentration analysis, and a loading concentration of 453,000 nuclei per mL was used for single nucleus RNA-seq (snRNA-seq) analysis of bladder tumors on DroNc-seq.

Barcoded beads (Chemgenes, cat #Macosko-2011-10(V+)) was washed, filtered through a 100  $\mu$ m cell strainer (Corning, cat #431752) followed by a 70  $\mu$ m cell strainer, and suspended in Drop-seq Lysis Buffer (6% Ficoll PM-400 (GE Healthcare, cat #17-0300-10), 0.2% Sarkosyl (Sigma Aldrich, cat #L7414), 0.02M EDTA (ThermoFisher, cat #AM9261), 0.2 M Tris Ph 7.5 (Invitrogen, cat #15567027), 0.05M DI-Dithiothreitol solution (Sigma Aldrich, cat #43816)) as described in Habib et al.<sup>7</sup>. The beads were counted using c-chip DHC-F01 counting chambers (NanoEnTek, cat #631-1096), the concentration was corrected to ~500,000 beads per mL and then they were ready for experiment run. For droplet

generation, nuclei and beads were applied for the system at flow rates of 20  $\mu$ L per min. Droplet Generation Oil for EvaGreen (BioRad QX200™, cat #1864006) was used to encapsulate the droplets at a flow rate of 120  $\mu$ L per min.

The same microfluidic system was used for Drop-Seq performed on T24 cells for comparison. T24 cells were isolated, trypsinized and washed as described in *Nuclei isolation for DroNc-seq*, and filtered through a 40  $\mu$ m cell strainer (Corning, cat #431750). The sNuc-seq Chip was replaced by a Droplet Chip 2 (100  $\mu$ m etch depth, fluorophilic, Dolomite Bio, cat #3200583) and the sample loop was adjusted from 6 m to 10 m in length. Furthermore, a cell concentration of 300,000 cells per mL and a bead concentration of 300,000 beads per mL were loaded for droplet generation at a flow rate of 30  $\mu$ L per min., and the flow rate for oil was increased to 200  $\mu$ L per min.

### **DroNc-seq and Drop-seq library preparation**

Droplet breaking, washes and reverse transcription (RT) was performed<sup>7</sup>. Beads were washed, treated with exonuclease I, resuspended in 1 mL H<sub>2</sub>O, and then counted<sup>7</sup>. Aliquots of 5,000 beads (~250 STAMPs) were amplified<sup>7</sup> using the following PCR program: 95 °C for 3 min., next four cycles of 98 °C for 20 s, 65 °C for 45 s, 72 °C for 3 min., then 9 cycles for Drop-seq and 12 cycles for DroNc-seq of 98 °C for 20 s, 67 °C for 20 s, 72 °C for 3 min., and finally 72 °C for 5 min. Supernatants from multiple PCR tubes with the same sample origin were pooled in a 1.5 mL Eppendorf tube, and 0.6× SPRI cleanup (Ampure XP, Beckman Coulter, cat #A63882) was performed. The cleanup procedure was repeated once for DroNc-seq samples. Quality assessment was performed on purified cDNA. Tagmentation and amplification was performed using Nextera XT DNA Library Preparation Kit (Illumina, cat #FC-131-1096) and 600 pg input of each sample. A final 0.6× SPRI cleanup and quality assessment was performed.

### **Sequencing of DroNc-seq libraries**

Single nuclei libraries were sequenced on the Illumina NovaSeq 6000 platform using a custom Read 1 primer (Read1CustomSeqB see **supplementary table 2**) and cycle parameters Read 1: 26 bases, Index read 1: 8 bases, Index read 2: 0 bases and Read 2: 75 bases. Read 1 reads through 12 bases of nuclei barcode, 8 bases of unique molecular identifier (UMI), 1 base (A/G/C), and then into the poly-T strand. According to recommendations from Illumina, 26 bases in read 1 were sequenced to ensure all Real-Time Analysis calculations are complete.

### Preprocessing of DroNc-seq and Drop-seq data

Processing of the FASTQ files was done as described in the Drop-Seq Core computational Protocol<sup>13</sup> with a few supplementary steps. First, the reads were sorted and only the ones where the barcodes were correctly formed, i.e. the molecular barcode was followed by a V (a A, C or G) and then the polyT were kept. Then the pipeline was run as described. To summarize: tag the biological read (read2) with the cell barcode and the UMI, filter reads with low quality barcodes, trim 5' primer sequence, trim 3' polyA, align the biological read with STAR, add gene/exon and other annotation tags and finally repair substitution errors or indel errors.

For each experiment, we then calculated the expression per barcode for all barcodes with a minimum of 150 genes expressed. The top ranked barcodes (either by the number of genes expressed or by the total read counts associated) were white-listed. The number depended on the theoretical number of single cells expected. We then created different tags where non-white-listed barcodes were changed to a white-listed barcode if the hamming distance between the two barcodes was less or equal to 2 (H2). Finally, for each tag, we recalculated the expression of each gene for all the barcodes in the white-list.

### snRNA-seq using 10x Chromium

For comparison of methods, T24 cells were also subjected to snRNA-seq using the 10x Chromium platform. Nuclei were isolated as described above (*Nuclei Isolation for DroNc-seq and 10x Chromium*), diluted to a concentration of 1,000 nuclei per  $\mu$ L and processed according to the 10x Chromium protocol, Chromium Next GEM Single Cell 3' Reagent Kits v3.1. Libraries were sequenced on an Illumina NovaSeq 6000 platform. Sequencing data were processed with CellRanger from 10x Genomics v7.0.0 using a pre-mrna reference (GRCh38-2020-A) and included introns.

### Comparison of single cell RNA-seq (Drop-seq) and single nuclei RNA-seq (DroNc-seq)

We compared the average transcriptomic profiles of single cells (Drop-seq) and single nuclei (DroNc-seq) from a T24 cell line by calculating the average log-transformed UMI counts and the Pearson correlation coefficient ( $R = 0.59$ ). We calculated the differential expression of genes between cells (Drop-seq) and nuclei (DroNc-seq) using the R software package Seurat<sup>20</sup> v3.1.0. The fraction of mapped reads for single cells (Drop-seq) and single nuclei (DroNc-seq and 10x Chromium) mapping to the exonic region, intergenic region, intronic region and mitochondrial region were also compared.

## Results

### Nuclei isolation

A laboratory protocol for snRNA-seq based on nuclei isolation was developed using human bladder tumors comprising both muscle invasive and non-muscle invasive disease (**figure 1**). The cell lysis conditions are paramount for successful isolation of nuclei with an intact nuclear membrane. To establish optimal conditions for this, different lysis buffers (IgePal and Nuclei EZ) and incubation times were tested in combination with different approaches for tissue and cell dissection; sectioning, semi-automated dissociation, manual dissociation with pestles, and semi-automated dissociation combined with manual dissociation with pestles (**supplementary figure 1, supplementary table 1**).

Dissection of the tissue by sectioning was most effective for isolation of a high number of undamaged nuclei relative to the amount of input tumor tissue ( $\text{mm}^3$ ), however, manual tissue dissection using pestles was also possible, but time-consuming and less robust. The Nuclei EZ lysis buffer was often too harsh on the tissue, leaving no or very few intact nuclei. Nuclei isolated with Nuclei EZ lysis buffer were often shrunken, had an uneven spiky circumference and were often rod-shaped. In contrast, IgePal lysis buffer with the detergent IGEPAL® CA-630 lysed only the plasma membrane leaving intact nuclei which had a smooth surface and a round to oval shape (**figure 2a-b**). Optimal incubation time in IgePal lysis buffer was 3-5 min. for non-muscle invasive bladder tumors and 5 min. for muscle invasive tumors. Prolonged incubation for more than 5 min. introduced ruptures of the nuclear membrane resulting in DNA leakage from the nuclei (**figure 2c**). Following lysis of the plasma membrane, nuclei were collected by centrifugation and two rounds of wash and filtering were performed to eliminate debris and residual cytoplasmic RNA. Single nuclei suspensions were stained with DAPI and imaged with fluorescence microscopy to ensure an intact nuclear membrane and no plasma membrane encapsulated cytoplasmic content (**figure 2d**). Furthermore, to ensure having enough nuclei for obtaining 3,000 STAMPs (single nucleus transcriptomes attached to microparticles, i.e. the result of a droplet with the transcriptome of a single nucleus attached to oligos of one bead) we isolated 145,000 nuclei. When approximately  $30 \text{ mm}^3$  tissue or more was used for nuclei isolation, we exceeded this threshold (**supplementary table 1**).

In summary, at least  $30 \text{ mm}^3$  tissue was used for nuclei isolation by sectioning on a cryostat. This was followed by incubation in IgePal lysis buffer for 3-5 min. to disrupt the outer cytoplasmic membrane and isolate the highest number of whole intact nuclei ( $>145,000$  nuclei) regardless of tumor stage and tissue structure.

### Bulk nuclei and bulk whole cell gene expression comparison

Prior to single nuclei analysis, we inspected whether the protocol for nuclei isolation changed the transcriptomic profile beyond the compartment restricted RNA species. We performed bulk mRNA-sequencing of the nuclear and cellular fractions from a bladder tumor and from a T24 human bladder cancer cell line. The nuclear fractions were isolated as described above and evaluated under a fluorescence microscope using DAPI to ensure properly isolated nuclei without remains of the cytoplasmic content. Nuclei, cells and tissue were lysed and bulk mRNA libraries were generated and sequenced. The bulk mRNA-sequencing data showed a relatively high correlation between gene expression from the nuclear and cellular fractions from both samples (Pearson  $R > 0.6$ , **figure 3**). Genes highly expressed in the cellular fraction for T24 but not in the corresponding nuclear fraction (marked by red dots) were all identified as mitochondrial genes as expected since these are expected to be removed during nuclear isolation (**figure 3**). These differences in mitochondrial gene expression were not identified for the tumor biopsy analysis, which could be caused by an overall higher cell cycle and energy requirement in pure cancer cells from the T24 cell line. These data suggest that the nuclei isolation protocol introduces limited bias to the transcriptome analysis.

### Nuclei concentration analysis

A nuclei concentration analysis was carried out to determine the appropriate nuclei concentration to avoid too many doublets, i.e. droplets that encapsulate two nuclei resulting in a mixture of their RNA and thereby a false RNA profile. To estimate this, a mixing experiment was carried out using nuclei isolated from two different cultured cell lines (T24 human bladder cancer cell line and NIH 3T3 murine cell line) mixed in ratio 1:1. Based on earlier reports<sup>7</sup>, two concentrations were tested: 450,000 nuclei per mL and 500,000 nuclei per mL. The identity of a particular nucleus was defined as human or murine origin if more than 95% of the transcripts harboring the same cell barcode mapped to the human or murine reference genome, respectively. A droplet was considered to have a mixed origin (i.e. a droplet containing one human nuclei combined with one murine nuclei) if less than 95% of the transcripts mapped to one of the reference genomes. The experiment revealed a doublet rate of 4.09% when using a concentration of 450,000 nuclei per mL, and a doublet rate of 20.00% when using a concentration of 500,000 nuclei per mL (**figure 4**). A concentration of approximately 453,000 nuclei per mL comparable to the concentration with the lowest murine-human doublet rate was used for DroNc-seq analysis of human bladder tumors.

### Gene expression concordance analysis for single nuclei and single cells

To investigate whether the transcriptional profiles of single nuclei were representative of whole cells, scRNA and snRNA-seq were applied on isolated T24 cells and nuclei, respectively. ScRNA-seq and snRNA-seq data was processed using the Macosko pipeline<sup>13</sup> with the addition of a few supplementary steps described in the methods under: *Preprocessing of DroNc-seq and Drop-seq data*. We compared the average expression of each gene (log-transformed counts) obtained for single nuclei and single cells to investigate if the nuclear transcriptomic profile contained a high degree of similarity to the cellular expression profile. We found a correlation of 0.59 between the average single cell and single nucleus transcriptome (**figure 5A**). Genes significantly higher expressed in nuclei (*NEAT1*, *MALAT1* and lncRNAs, *PAX8-AS1* and *XIST*) or cells (*MT-RNR2*, *RPS3*, *RPL8*, *RPL11*, and *RPL19*) were consistent with the compartment restricted RNA species.

We also compared the fraction of reads mapping to exonic, intronic and mitochondrial regions for scRNA-seq (Drop-seq) and snRNA-seq data obtained from two different platforms, DroNc-seq and 10x Chromium. As expected, a large fraction of reads (74.57%) mapped to exons for single cells (Drop-seq), whereas the corresponding fractions of reads mapping to exons (37.19% for DroNc-seq and 27.6% for 10x Chromium) was lower for single nuclei (**figure 5B**). Nonetheless, a low fraction of reads mapped to introns (7.18%) for single cells (Drop-seq) compared to single nuclei (36.58% for DroNc-seq and 59.9% for 10x Chromium) (**figure 5B**). The observed fractions of intron- and exon-mapped reads in the nuclei may reflect the maturation process of RNA in the nuclei<sup>12</sup>. Finally, only a small fraction of reads mapping to mitochondrial genes were observed for cells (3.05%) and close to none (<0.11%) for single nuclei emphasizing complete isolation of single nuclei without mitochondrial contribution.

### Discussion

Here we describe a protocol for snRNA-seq including a robust procedure for gentle nuclei isolation from fresh frozen tissue using dissection of tissue by sectioning and incubation in IgEPal lysis buffer. Comparison of gene expression profiles from nuclei and cells showed a high concordance and genes known to be specifically expressed in different cellular compartments were identified<sup>14,15</sup>. The fraction of reads obtained from either nuclei or cells were enriched according to the origin of the RNA analyzed, which is congruent with previous studies<sup>7,12</sup>.

The majority of previous studies have investigated single cells from fresh tissue, which might cause a challenge in laboratory workflow and lack of information on the samples being analyzed - especially in clinical studies. It is not possible to analyze single cells isolated from frozen biobanked material since the RNA integrity in biopsies decreases drastically if the

sample is thawed after it has been snapfrozen because of RNase activity<sup>16</sup>. This stresses the advantage that snRNA-seq has over scRNA-seq because already biobanked material and tissue difficult to dissociate into single cells can be analyzed. Explorative studies can utilize this and be designed for patients with well described clinical and histopathological information and known clinical outcomes.

A previous study comparing scRNA-seq and snRNA-seq showed that fewer immune cells were recovered from frozen mouse kidney tissue compared to fresh tissue (0.73% and 6.03%, respectively) with an underrepresentation of T-, B-, and natural killer-lymphocytes in their single nuclei study<sup>17</sup>. However, in another study, Gouin et al. performed snRNA-seq on fresh frozen bladder tumor samples and identified a fraction of immune cells (5%) comprising T-cells, dendritic cells, macrophages, and B-cells defined by classic immune marker genes<sup>4</sup>. A third study on human cervical squamous cell carcinoma also performing snRNA-seq identified a diverse population of immune cells as well<sup>18</sup>. Although they identify immune cells, these studies might underestimate the true fraction of immune cells present in their natural conditions after all. It is unknown whether the variation in immune populations identified is tissue specific, caused by heterogeneity within the tissue or caused by preservation methods.

In comparison to DroNc-seq, 10x genomics has also developed a droplet-based platform (Chromium) for single cell and single nucleus analysis. A comparative study of scRNA-seq and snRNA-seq methods showed that 10x Chromium has a higher performance with a notable increase in data per nuclei compared to the DroNc-seq system<sup>10</sup>. This could be due to better error suppression in nuclei barcodes and/or the utilization of elastic beads. Furthermore, the capture rate of 10x Chromium is 60% whereas the capture rate of DroNc-seq is 5%<sup>7</sup>, putting a higher demand on the amount of input material needed. However, while the 10x Chromium platform is less time-consuming and a more standardized system, the DroNc-seq system is more cost-effective, which is favorable for high-throughput studies that include multiple samples.

In conclusion, we successfully optimized a robust and reproducible protocol for nuclei isolation applicable across various tumor stages and tumor morphology structures. This nuclei isolation protocol combined with our optimized library preparation for next generation sequencing provides the full workflow for snRNA-seq of human bladder tumors, from frozen tumor biopsies to data ready for analysis.

## Acknowledgements

We would like to thank all technical personnel at Department of Molecular Medicine and Department of Urology and Oncology, Aarhus University Hospital, for sample handling and

processing. Thanks to GenomeDK, which was used for analysis. Some of the computing for this project was performed on the GenomeDK cluster. We would like to thank GenomeDK and Aarhus University for providing computational resources that contributed to these research results.

### Competing interests

Lars Dyrskjøt has sponsored research agreements with C2i, AstraZeneca, Natera, Photocure, and Ferring; has an advisory/consulting role at Ferring and UroGen; and is Chairman of the Board in BioXpedia A/S.

Jørgen Bjerggaard Jensen is proctor for Intuitive Surgery; is a member of advisory board for Olympus Europe, Ambu, Cepheid, and Ferring; and has sponsored research agreements with Medac, Photocure ASA, Cepheid, and Ferring.

### Data availability

The raw sequencing data generated in this study are not publicly available as this compromise patient consent and ethics regulations in Denmark. Processed non-sensitive data are available upon reasonable request from the corresponding author.

### Author contributions

Conceptualization S.S.S., I.N., L.D.; Data Curation S.S.S., S.V.L., P.L., M.K.; Formal Analysis S.S.S., S.V.L., P.L.; Funding Acquisition L.D.; Investigation S.S.S., I.N.; Methodology S.S.S., I.N., L.D.; Project Administration L.D.; Resources J.B.J., L.D.; Supervision L.D.; Visualization S.S.S., M.K.; Writing – Original Draft: S.S.S., I.N., S.V.L., L.D.; Writing – Review & Editing: all authors.

### Funding information

Independent Research Fund Denmark, The Novo Nordisk Foundation, Aarhus University (AUFF NOVA), The Leo & Anne Albert Institute for Bladder Cancer Care and Research.

### Figure legends

**Figure 1 Experimental workflow.** 1) Nuclei isolation through tissue dissection by sectioning and incubation in IgePal lysis buffer. 2) Evaluation of DAPI-stained nuclei using fluorescence microscopy. 3) Nuclei encapsulation using DroNc-seq. 4) Construction of libraries. 5) Next generation sequencing of libraries. 6) Data analysis (created with BioRender.com).

**Figure 2 Isolated DAPI-stained nuclei.** A) T24 cell line nuclei. B) Human bladder tumor nuclei. C) DNA leaking from human bladder tumor nuclei. D) Incomplete nuclei isolation of human bladder tumor with remains of the cytoplasmic membrane. Nuclei are stained with DAPI and evaluated through a fluorescence microscope.

**Figure 3 Concordance between gene expression profiles for nuclei and cells.**

Scatterplot of gene expression [ $\log(\text{counts}+1)$ ] from fractions of cellular and nuclear bulk mRNA from A) T24 human bladder cancer cell line and B) human muscle-invasive bladder tumor. Pearson correlation was used to determine the correlation coefficient R and p-value. Red dots indicate deviating genes highly expressed in one fraction but not the other.

**Figure 4 Nuclei concentration analysis.** Nuclei identity of the mixing experiment using a nuclei concentration of A) 450 nuclei per  $\mu\text{L}$  and B) 500 nuclei per  $\mu\text{L}$ . A) 204 unique murine nuclei, 179 unique human nuclei, and 8 mixed nuclei were identified. B) 157 unique murine nuclei, 149 unique human nuclei, and 34 mixed nuclei were identified. Blue dots: droplets with murine nuclei. Red dots: droplets with human nuclei. Black dots: droplets with human and mouse nuclei. Cut-off values: min. 1 read per gene, min. 200 genes per nuclei, >95% reads must map to the human or murine reference genome, respectively, to define a cell as unique.

**Figure 5 Comparison of gene expression in single nuclei and single cells.** A) Scatterplot comparing average gene expression (log-transformed) for single nucleus and single cell data from T24 human bladder cancer cell line. Pearson correlation was used to determine the correlation coefficient R and p-value. Selected genes significantly expressed in either cells or nuclei are marked in red. B) Fraction of reads mapping to exonic, intronic, intergenic and mitochondrial regions (out of the reads mapped to the genome) for T24 cells (Drop-seq) and T24 nuclei (10x Chromium and DroNc-seq).

**Supplementary Figure 1 Experimental workflows tested for optimization of nuclei isolation.** Three types of tissue conditions ( $n = 83$ ), fresh, fresh frozen and dry frozen, was tested in combination with various approaches for tissue dissection by sectioning, manual dissection (pestles), semi-automated dissection (gentleMACS), and semi-automated dissection (gentleMACS) combined with manual dissection (pestles). These combinations were further combined with either IgEPal lysis buffer or Nuclei EZ lysis buffer. Beneath each workflow, it is stated how many experiments have been performed and how large the success rate was (experiments obtaining >145,000 nuclei) (created with BioRender.com).

**Supplementary Table 1 Experimental overview of workflows tested during optimization of nuclei isolation.**

**Supplementary Table 2 Primers used throughout DroNc-seq and Drop-seq experiments.** V: A, C or G. r indicates a ribose-phosphate backbone. \* indicate a phosphorothioate bond between two bases. TSO: template switch oligo.

**References**

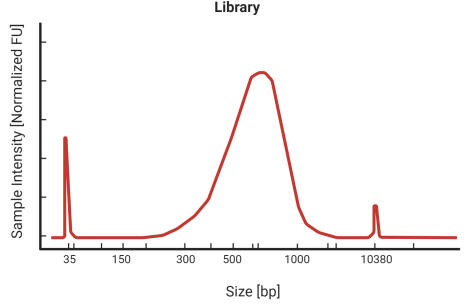
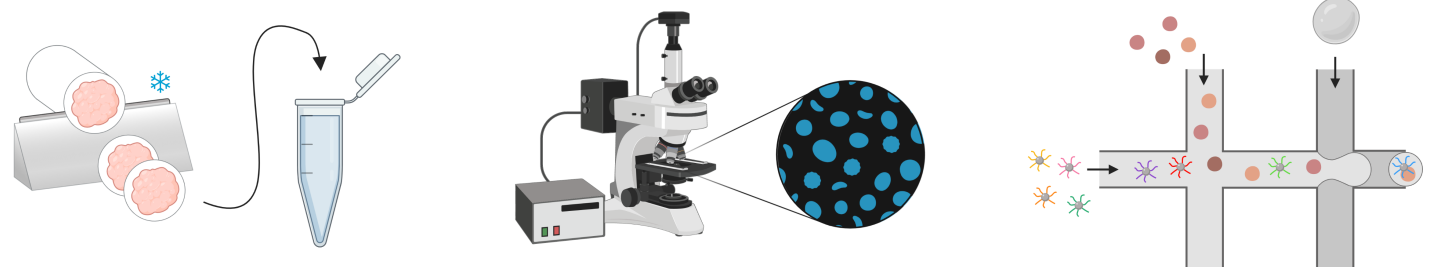
1. Young, M. D. *et al.* Single-cell transcriptomes from human kidneys reveal the cellular identity of renal tumors. *Science* **361**, 594–599 (2018).
2. Tirosh, I. *et al.* Dissecting the multicellular ecosystem of metastatic melanoma by single-cell RNA-seq. *Science* **352**, 189–196 (2016).
3. You, S. *et al.* Characterizing molecular subtypes of high-risk non-muscle-invasive bladder cancer in African American patients. *Urologic Oncology: Seminars and Original Investigations* (2022) doi:10.1016/J.UROLONC.2022.04.013.
4. Gouin, K. H. *et al.* An N-Cadherin 2 expressing epithelial cell subpopulation predicts response to surgery, chemotherapy and immunotherapy in bladder cancer. *Nature Communications* **2021 12:1** 12, 1–14 (2021).
5. Giladi, A. & Amit, I. Single-Cell Genomics: A Stepping Stone for Future Immunology Discoveries. *Cell* **172**, 14–21 (2018).
6. Giustacchini, A. *et al.* Single-cell transcriptomics uncovers distinct molecular signatures of stem cells in chronic myeloid leukemia. *Nat. Med.* **23**, 692–702 (2017).
7. Habib, N. *et al.* Massively parallel single-nucleus RNA-seq with DroNc-seq. *Nat. Methods* **14**, 955–958 (2017).
8. Macosko, E. Z. *et al.* Highly parallel genome-wide expression profiling of individual cells using nanoliter droplets. *Cell* **161**, 1202–1214 (2015).
9. Enyedi, B. & Niethammer, P. Nuclear membrane stretch and its role in mechanotransduction. <https://doi.org/10.1080/19491034.2016.1263411> **8**, 156–161

(2017).

10. Ding, J. *et al.* Systematic comparison of single-cell and single-nucleus RNA-sequencing methods. *Nat. Biotechnol.* **38**, 737–746 (2020).
11. Baghirova, S., Hughes, B. G., Hendzel, M. J. & Schulz, R. Sequential fractionation and isolation of subcellular proteins from tissue or cultured cells. *MethodsX* **2**, e440–e445 (2015).
12. Selewa, A. *et al.* Systematic Comparison of High-throughput Single-Cell and Single-Nucleus Transcriptomes during Cardiomyocyte Differentiation. *Sci. Rep.* **10**, 1535 (2020).
13. Nemesh. *Dropseq Core Computational Protocol*.  
[https://raw.githubusercontent.com/broadinstitute/Drop-seq/v2.4.0/doc/Drop-seq\\_Alignment\\_Cookbook.pdf](https://raw.githubusercontent.com/broadinstitute/Drop-seq/v2.4.0/doc/Drop-seq_Alignment_Cookbook.pdf).
14. Gupta, A. *et al.* Characterization of transcript enrichment and detection bias in single-nucleus RNA-seq for mapping of distinct human adipocyte lineages. *Genome Res.* **32**, 242–257 (2022).
15. Gao, R. *et al.* Nanogrid single-nucleus RNA sequencing reveals phenotypic diversity in breast cancer. *Nature Communications* **2017 8:1** 8, 1–12 (2017).
16. Ma, Y., Dai, H. & Kong, X. Impact of warm ischemia on gene expression analysis in surgically removed biosamples. *Anal. Biochem.* **423**, 229–235 (2012).
17. Denisenko, E. *et al.* Systematic assessment of tissue dissociation and storage biases in single-cell and single-nucleus RNA-seq workflows. *Genome Biol.* **21**, 1–25 (2020).
18. Ou, Z. *et al.* Single-Nucleus RNA Sequencing and Spatial Transcriptomics Reveal the Immunological Microenvironment of Cervical Squamous Cell Carcinoma. *Adv. Sci.* e2203040 (2022).
19. Patro, R., Duggal, G., Love, M. I., Irizarry, R. A. & Kingsford, C. Salmon provides fast and bias-aware quantification of transcript expression. *Nat. Methods* **14**, 417–419 (2017).
20. Stuart, T. *et al.* Comprehensive Integration of Single-Cell Data. *Cell* **177**,

1888–1902.e21 (2019).

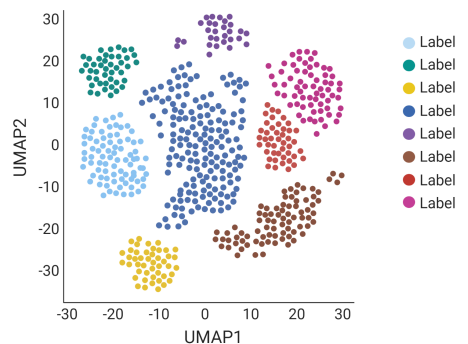
Figure 1



4. Library Construction



5. Next Generation Sequencing



6. Data Analysis

Figure 2

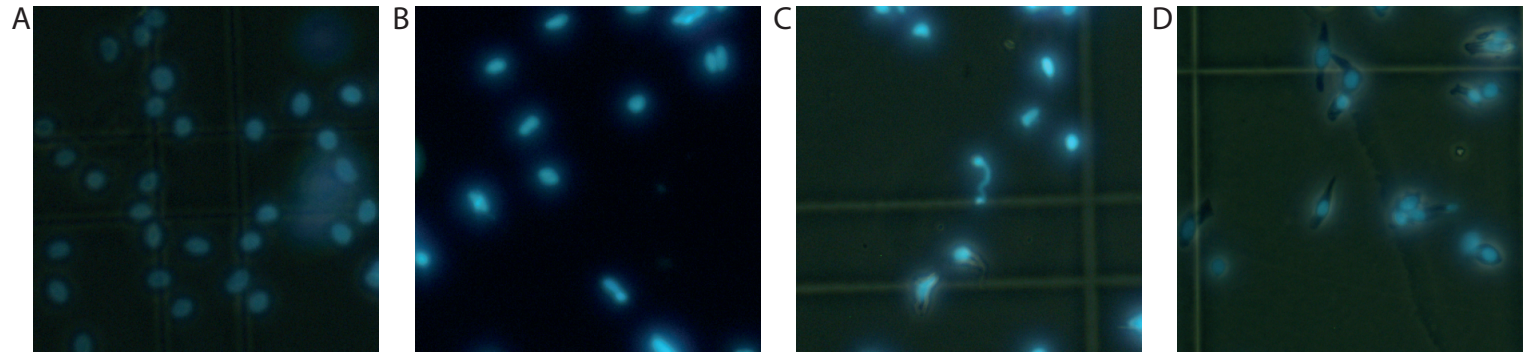


Figure 3

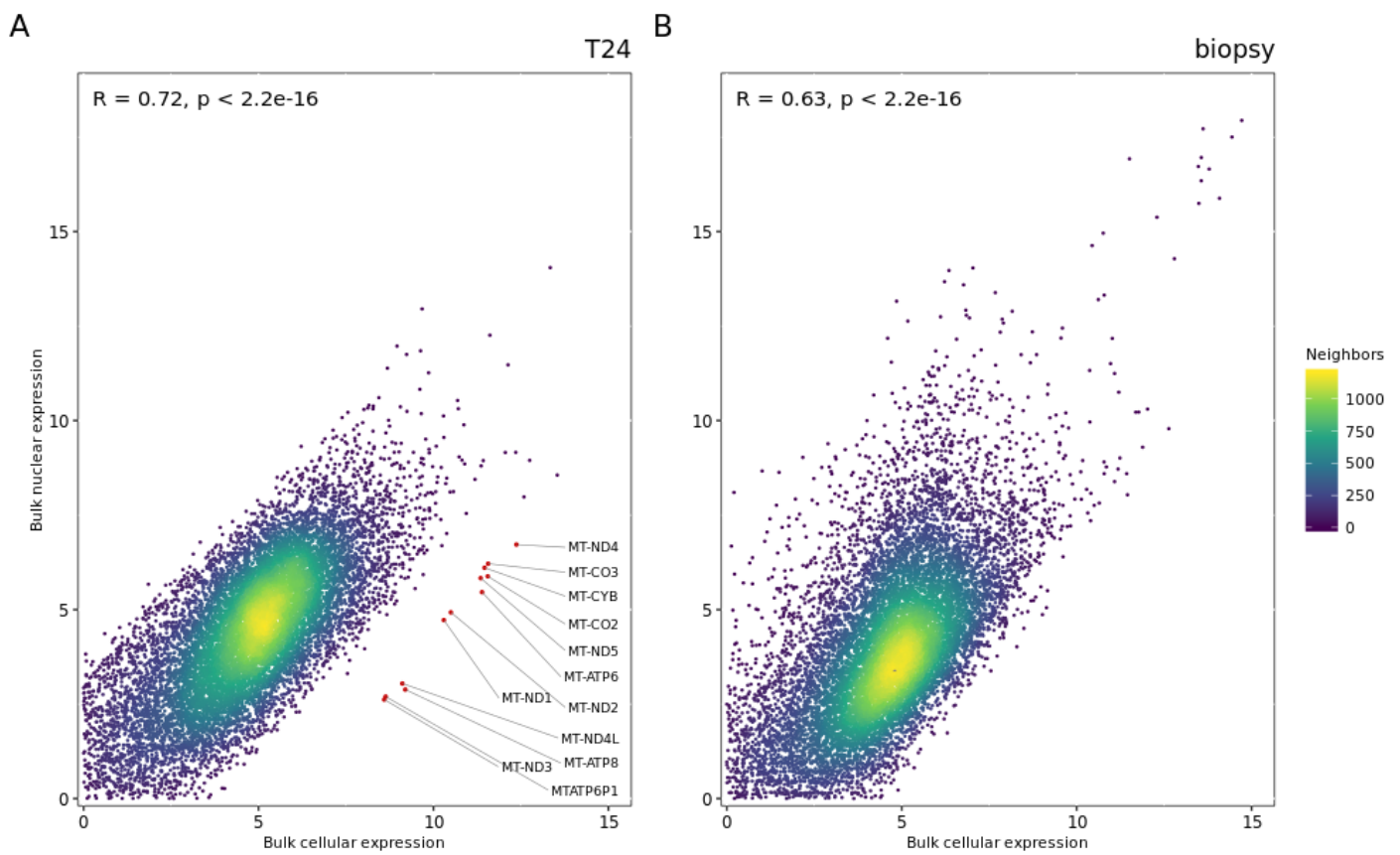


Figure 4

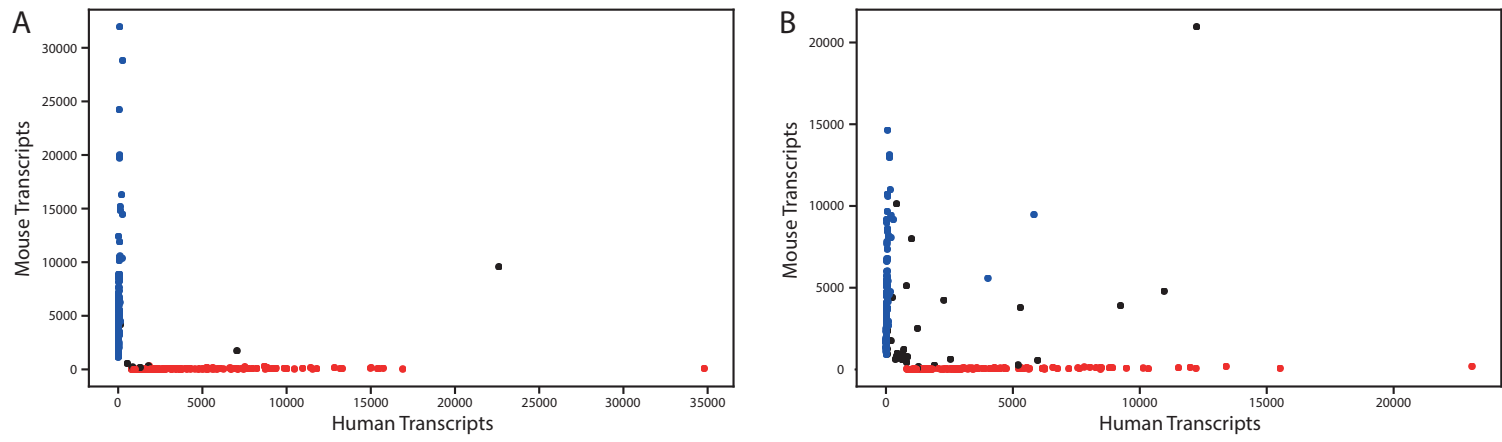


Figure 5

